Antiferromagnetic interlayer coupling in diluted magnetic thin films with RKKY interaction

Karol Szałowski* and Tadeusz Balcerzak
Department of Solid State Physics, University of Łódź, ulica Pomorska 149/153, 90-236 Łódź, Poland
(Received 14 January 2009; revised manuscript received 4 April 2009; published 24 June 2009)

We study a model thin film containing diluted bilayer structure with the Ruderman-Kittel-Kasuya-Yosida long-range interaction. The magnetic subsystem is composed of two magnetically doped layers, separated by an undoped nonmagnetic spacer, and placed inside a wider film modeled by a quantum well of infinite depth. We focus our study on the range of parameters for which the antiferromagnetic coupling between the magnetic layers can be expected. The critical temperatures for such system are found and their dependence on magnetic layer thickness and charge-carrier concentration is discussed. The magnetization distribution within each magnetic layer is calculated as a function of layer thickness. The external field required to switch the mutual orientation of layer magnetizations from antiferromagnetic to ferromagnetic state is also discussed.

DOI: 10.1103/PhysRevB.79.214430 PACS number(s): 75.70.−i, 75.50.−y, 75.30.−m

I. INTRODUCTION

The phenomenon of mutual coupling of magnetic layers separated by a nonmagnetic medium has been of great interest since its discovery in Fe/Cr structure,[1] both due to its immense application potential and the highly nontrivial physical background.[2–8] In parallel to studies of metallic systems, the progress in the field of thin films made of diluted magnetic semiconductors (DMSs), such as the most representative (Ga,Mn)As, offers some new possibilities to study the diluted magnetic systems with confined geometry. Such materials are promising from the future spintronics point of view[9] since they can assure integrability of novel spin-current devices with conventional structures of semiconductor-based electronics.[10] In DMS an indirect coupling between localized spins mediated by charge carriers is of paramount importance for the possibility of magnetic ordering. The Ruderman-Kittel-Kasuya-Yosida (RKKY) interaction mechanism was suggested to describe the properties of quantum-well-based DMS systems a decade ago.[11]

The problem of interlayer coupling in multilayers and superlattices of DMS has been subject to various theoretical studies. However, let us notice that the theoretical approaches have been dedicated mainly to multilayers and superlattices, while the structures based on bi- or trilayer geometry have attracted less attention. Giddings *et al.*[12] performed some calculations within a single parabolic band approximation for $\mathbf{k}\cdot\mathbf{p}$ method and local density approximation to study the possibility of the appearance of antiferromagnetic (AF) interlayer coupling in the superlattices of (Ga,Mn)As. They concluded that the minimization of spacer thickness accompanied with relatively short superlattice period is advantageous for a strong coupling. This problem has also been investigated by Sankowski and Kacman,[13] who found in their tight-binding-based study a relative insensitivity of the coupling energy to the magnetic layer thickness. A noticeable range of parameters favoring the AF interlayer interaction has been identified. The self-consistent mean-field calculations for multilayers were also performed by Jungwirth *et al.*[14] The study of Rodrigues *et al.*[15] was devoted to the distribution of charge and spin polarization in the multilayer. On the other hand, several works have been focused on the quantum-well-based systems containing two layers separated by a nonmagnetic spacer. These involve mainly the Monte Carlo (MC)-based studies of Boselli *et al.*[16,17]

Numerous experimental works evidenced the fact that two magnetically doped layers can be indirectly coupled for some interlayer distances. The effect has been studied both in magnetic bilayers and in multilayer systems. For example, the results of Sadowski *et al.*[18] proved the possibility of magnetic ordering in (Ga,Mn)As layers thinner than 50 Å in multilayer geometry, and such ferromagnetism had a tendency to vanish if the nonmagnetic spacer was more than 10 ML thick. A distinct coupling has been observed in (Ga,Mn)As/GaAs trilayers by means of magnetotransport and magnetization process studies by Akiba *et al.*[19] The quantitative analysis was performed there yielding the ferromagnetic (F) interlayer couplings close to 0.1 $\mathrm{mJ/m^2}$ for the nonmagnetic spacer up to 10 ML thick. On the other hand, the ferromagnetic coupling observed by Chiba *et al.*[20] was one order of magnitude weaker. The ferromagnetic resonance in (Ga,Mn)As heterostructures investigated by Dziatkowski *et al.*[21] indicated that the layers were uncoupled for nonmagnetic spacers thicker than 32 ML, while for 10 ML a full coupling took place. The superlattice structures of the same DMS have been investigated by Mathieu *et al.*,[22] where the critical temperature was found to oscillate with the spacer thickness (up to 9 ML), and thus the presence of interlayer coupling was deduced. Short-period superlattices formed the basis of neutron reflectivity studies of Szuszkiewicz *et al.*,[23] who confirmed the ferromagnetic-only interlayer coupling (mainly for 6 ML spacer). In the work of Kirby *et al.*[24] neutron reflectometry and magnetization curve studies of trilayer structures were performed in which the magnetization of top and bottom layer has been resolved. This indicated distinct ferromagnetic coupling through a spacer of large thickness (about 20 ML). It was also excluded in the paper of Kirby *et al.*[24] that the spacer has been plagued by diffusion of the magnetic impurities leading to direct coupling mechanism. However, it should be mentioned that the diffusion of Mn impurities into the spacer is possible, as it has been proven experimentally by STM methods.[25] On the other hand, the results of Ge *et al.*[26] show the difference of critical temperatures for top and bottom layers in a trilayer system, a differ-

ence which had a tendency to vanish when the nonmagnetic spacer thickness was reduced (and a single common transition temperature has been observed for the spacer of about 10 ML thick). Let us note that in that paper it has been stated that the sign of coupling energy might be spatially inhomogeneous—either F or AF for various areas on the surface of the sample, which was deduced from the observation of planar Hall effect. However, it was not until last year that the AF coupling between layers in (Ga,Mn)As/GaAs:Be was clearly observed by means of dc magnetometry as well as neutron reflectivity studies performed by Chung *et al.*[27] The critical temperature of the system was about 50 K. All the discussed interlayer coupling signatures have been assigned to the carrier-mediated interaction mechanism.

The above results encourage further search for the possibility of obtaining AF interlayer carrier-mediated coupling. Therefore, it seems purposeful to devote a theoretical study to the trilayer structure, which can be formed by two magnetic layers immersed in the thin film and separated by a nonmagnetic spacer, with the aim to discover some unique properties of RKKY interaction in the ultrathin film. From the practical point of view it is interesting to find a range of carrier concentrations and geometric characteristics with AF coupling. In particular, the influence of the magnetic layer thickness on the coupling energy and the critical temperature of the system poses an important question. In order to have a deeper insight, also the spatial distribution of magnetization within the magnetic layers appears worthwhile to examine.

For the above reasons, in this paper our purpose is to study a model trilayer system with the RKKY interaction. The theoretical model is based on the quantum-well approach to the thin film for which the RKKY exchange coupling has been rederived. The numerical calculations have been performed for some realistic material constants, typical of DMS systems.

II. THEORETICAL MODEL

We consider a model thin film consisting of n monolayers, where some of the planes can be doped with magnetic impurity ions. The doped planes form two magnetic layers, separated by a nonmagnetic spacer (Fig. 1). Each magnetic plane consists of n_L doped atomic planes, while the undoped spacer has the thickness of n_S monolayers. As a consequence, the inequality $2n_L+n_S \leq n$ must hold. The film possesses fcc structure and its surface orientation is (001). The localized spins situated in the lattice site $(\mathbf{r}_i, z_\nu)$ can be shortly denoted by $\mathbf{S}_{i,\nu}$, where ν is one of the atomic planes whose position is given by $z_\nu=(\nu-1/2)d$, and $\mathbf{r}_i$ is the vector in the plane. d is the thickness of a single monolayer, and the total thickness of the film is $D=nd$. The choice of structure is motivated by the fact that the ultrathin films of (Ga,Mn)As are most often grown with this surface orientation, on (001)GaAs substrate. Our film constitutes a quantum well of infinite depth in z direction for the charge carriers. Confining electrons in such a quantum-well results in discretization of the Fermi surface, which for such a system is composed of a finite number of circular "slices," each of them corresponding to one two-dimensional (2D) energy subband (indexed by an integer τ).

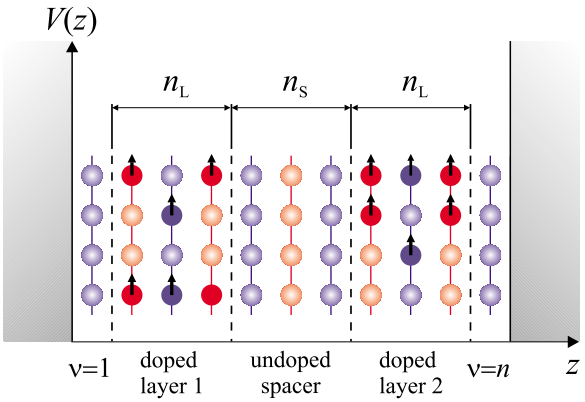

FIG. 1. (Color online) Schematic cross section of an ultrathin film containing two magnetically doped layers. In this figure the total thickness of the film amounts to $n=11$, whereas the thickness of each magnetic layer is $n_L=3$ and the thickness of nonmagnetic spacer is $n_S=3$.

Therefore, the dispersion relation for charge carriers takes the form of

$$E_{\mathbf{k},\tau} = \frac{\hbar^2}{2m}\left(\mathbf{k}^2 + \frac{\pi^2}{D^2}\tau^2\right), \tag{1}$$

where $\mathbf{k}$ is a 2D in-plane wave vector.

For the free-electron model, the perturbation Hamiltonian describing the exchange interaction between the single localized magnetic moment at $(\mathbf{r}_i, z_\nu)$ and the free charge carrier at $(\mathbf{r}, z)$ is assumed to be in the following form:

$$\mathcal{H} = -Ap(\mathbf{r}, z)S^z_{i,\nu}s^z(\mathbf{r}, z), \tag{2}$$

where A is the exchange constant,

$$p(\mathbf{r}, z) = \frac{1}{\sigma^3(2\pi)^{3/2}} e^{-((r-r_i)^2+(z-z_\nu)^2)/2\sigma^2}, \tag{3}$$

and $s^z(\mathbf{r}, z)$ is the z component of the free-electron spin in the $(\mathbf{r}, z)$ point of the film.

We emphasize the fact that the selected "diffused" contact potential $p(\mathbf{r}, z)$ differs from the usual Dirac delta function since it has a nonzero dispersion σ^2. The contact potential frequently used in derivation of RKKY indirect exchange integral is reproduced in the limit $\sigma \to 0$. Such a form of formula (3) is further substantiated by the fact that the localized magnetic moments originate from the d-type electronic orbitals which possess some spatial extension. Note that such a potential has already been applied in studies of bulk DMS.[28–30]

The influence of "diffusion" of the contact potential on the resulting RKKY coupling integral in one-dimensional (1D), 2D, and three-dimensional (3D) systems has recently been studied in Ref. 31. The studies resulted in obtaining a finite value of RKKY integral for $\mathbf{r}=0$ in 2D and 3D case. The importance of this result has first been noticed for discrete 3D systems since the presence of divergence at $\mathbf{r} \to 0$ leads to some divergent self-energy corrections.[28] However, it must be emphasized that in studies of ultrathin films the acceptance of a finite σ value is necessary, even if we do not

require the self-energy to be finite. The reason is that the RKKY exchange integral derived on the basis of the contact potential with $\sigma=0$ is divergent for arbitrary z when $r=0$, i.e., in the direction perpendicular to the film plane, even though the distance between the interacting spins is nonzero. This fact precludes the further studies on the total energy of the discrete system if $\sigma=0$.

By applying the second-order perturbation calculus we obtain the RKKY exchange integral between the localized spins separated by the distance $\Delta r=|\mathbf{r}_i-\mathbf{r}_j|$ in the plane of the film, and $\Delta z=|z_\nu-z_\mu|$ in the direction perpendicular to the film surface. The integral has the form of

$$J(\Delta r,\Delta z)=C\left(\frac{a}{d}\right)^4\frac{\pi}{4n^2}\int_0^{+\infty}dy\left[yJ_0\left(y\frac{\Delta r}{d}\right)e^{-(\sigma/d)^2y^2}\times\sum_{l=-\infty}^{+\infty}\frac{\chi_{l,y}}{\chi_0}\cos\left(\frac{2\pi}{n}\frac{\Delta z}{d}l\right)\phi^2(l)\right]. \tag{4}$$

In the above formula, $\phi(l)$ is the Fourier transform of the z-dependent part in the interaction potential $p(\mathbf{r},z)$, and it can be presented as $\phi(l)=\exp(i\frac{2\pi}{D}l\sigma)$ for $\sigma/d\ll 1$.[32] The symbol $\chi_{l,y}$ denotes the paramagnetic susceptibility of the electrons in the ultrathin film, which has been derived elsewhere,[33,34] while χ_0 is the Pauli susceptibility of 2D system. The energy constant C in Eq. (3) is given by $C=2mA^2/\pi h^2a^4$, where a is the lattice constant.

The Hamiltonian for the system under consideration is assumed to be of Ising type with the long-range exchange interaction $J(\Delta r,\Delta z)$,

$$\mathcal{H}=-\sum_{\langle i,\mu;j,\nu\rangle}J(\Delta r,\Delta z)\xi_{i,\mu}\xi_{j,\nu}S^z_{i,\mu}S^z_{j,\nu}+g_{\mathrm{eff}}\mu_B B\sum_{i,\mu}\xi_{i,\mu}S^z_{i,\mu}. \tag{5}$$

The above Hamiltonian includes the Zeeman term for the system embedded in an uniform external field B. The localized spins reveal the effective gyromagnetic factor $g_{\mathrm{eff}}=g_S+g_e(\pi Am\tau_{\mathrm{F}}/h^2D)$,[35] where g_S and g_e are the gyromagnetic factors of localized spins (without RKKY interaction) and the free electrons, respectively. τ_{F} is the number of subbands, splitted due to the discretization of Fermi surface in thin film.[36]

In order to describe a site dilution in the system we make use of the Edwards operators $\xi_{i,\mu}$,[37] which possess two eigenvalues: 1 when the site (i,μ) is occupied by a magnetic impurity or 0 otherwise. In this paper, for simplicity, we will neglect the correlations of $\xi_{i,\mu}$ operators; i.e., the Warren-Cowley short-range-order parameter[38] is assumed here to be 0. It means that the occupation of lattice sites by the impurity ions in doped planes is completely random. As a consequence, the configurational averages read as $\langle\xi_{i,\mu}\rangle_r=x$ and $\langle\xi_{i,\mu}\xi_{j,\nu}\rangle_r=x^2$ if sites (i,μ) and (j,μ) belong to the magnetically doped atomic planes and vanish otherwise, whereas x is the magnetic dopant concentration. In further considerations it will be assumed that indices μ and ν run only over the magnetically doped atomic planes.

By taking thermodynamic and configurational average of Hamiltonian (5) for the temperature $T\to 0$, we obtain the ground-state enthalpy $H=\langle\mathcal{H}\rangle$ of the magnetic system under consideration. The enthalpy can be conveniently written as a sum of contributions originating from the energy of spin interactions within a single magnetic layer, the energy of interactions between two layers, and the interaction with an external field. For the temperature $T\to 0$ the magnetization in each atomic plane ν constituting a specified magnetic layer is the same, for instance, $\langle S^z_{i,\mu}\rangle=m_1=\pm S$ for the first layer and $\langle S^z_{i,\mu}\rangle=m_2=\pm S$ for the second one; i.e., both layers are fully polarized (ferro- or antiferromagnetically each to the other). As a consequence, the total enthalpy per one site in a doped atomic plane reads as

$$\frac{H}{N}=\frac{E_{\mathrm{intra}}}{N}+\frac{E_{\mathrm{inter}}}{N}-xn_Lg_{\mathrm{eff}}\mu_BB(m_1+m_2). \tag{6}$$

Since each layer is ferromagnetically ordered inside, the energies of intralayer and interlayer interactions can be written in the form of

$$\frac{E_{\mathrm{intra}}}{N}=-x^2S^2\mathcal{E}_{\mathrm{intra}} \tag{7}$$

and

$$\frac{E_{\mathrm{inter}}}{N}=-x^2m_1m_2\mathcal{E}_{\mathrm{inter}}. \tag{8}$$

In the above equations we denoted the appropriate lattice sums by

$$\mathcal{E}_{\mathrm{intra}}=n_L\mathcal{E}(0)+\sum_{\nu=1}^{n_L-1}(n_L-\nu)\mathcal{E}(\nu) \tag{9}$$

and

$$\mathcal{E}_{\mathrm{inter}}=n_L\mathcal{E}(n_L+n_S)+\sum_{\nu=1}^{n_L-1}(n_L-\nu)[\mathcal{E}(n_L+n_S+\nu)+\mathcal{E}(n_L+n_S-\nu)], \tag{10}$$

where

$$\mathcal{E}(\omega)=\sum_k z_k^{\mathcal{P}(\omega)}J(r_k^{\mathcal{P}(\omega)},\omega d). \tag{11}$$

The logic index $\mathcal{P}(\omega)$ stands for the parity of ω, which refers to the fact that in (001)-oriented fcc-based thin film, the subsequent atomic planes are mutually shifted parallel to the surface. This requires two sets of coordination zones radii r_k and coordination numbers z_k to be used: one if both spins are situated in the same plane (or in the planes separated by an even number of interplanar distances), $\mathcal{P}(\omega)=$"even" and the other for the situation when both spins lie in the planes separated by an odd number of interplanar distances, $\mathcal{P}(\omega)=$"odd". Both sets of numbers have to be determined numerically for the assumed crystallographic structure. $\mathcal{P}(0)$ requires the point $(\mathbf{r}=0,\ z=0)$ to be excluded from summation.

In the system considered, the area per one site in the (001) atomic plane is $S=a^2/2$ so that the interlayer coupling en-

ergy per unit area of the film is $2x^2S^2\mathcal{E}_{\text{inter}}/a^2$. Let us note that the interlayer coupling energy is often defined as the difference in energies of the system for ferromagnetic ($E^{\uparrow\uparrow}$) and antiferromagnetic ($E^{\uparrow\downarrow}$) alignment of magnetic moments in these layers. In our notation such a difference is $(E^{\uparrow\uparrow}-E^{\uparrow\downarrow})/N=-2x^2S^2\mathcal{E}_{\text{inter}}$.

When we consider the magnetic monoatomic layers with the thickness $n_L=1$, expressions (9) and (10) reduce only to the first terms, without summation over ν.[32] On this basis, as a special case, we can study the interplanar coupling energy for two magnetically doped planes as a function of their separation for different total thicknesses of the film.

In general, for nonzero temperature, the magnetizations m_μ per one magnetic impurity in each magnetically doped plane are not equal for all μ so that some spatial magnetization profile is present in the magnetic layers. In the molecular-field approximation (MFA), these magnetizations can be obtained as the solutions to the set of $2n_L$ coupled self-consistent equations,

$$m_\mu = S\mathcal{B}_S\left(S\frac{\Lambda_\mu}{k_BT}\right). \tag{12}$$

It should be kept in mind that the index μ here runs only over the magnetically doped monolayers. $\mathcal{B}_S(x)$ is the Brillouin function for spin S, and the molecular field acting on a given spin in the layer μ is

$$\Lambda_\mu = x\sum_\nu \mathcal{E}(|\mu-\nu|)m_\nu. \tag{13}$$

The summation over ν in Eq. (12) is restricted to the magnetically doped atomic planes.

From linearization of the above set of equations for magnetization, in vicinity of the critical point, we obtain the critical temperature of a second-order phase transition. It is given by the largest real root of the equation,

$$\det \mathcal{J}=0, \tag{14}$$

where the matrix $\mathcal{J}$ is of size $2n_L\times 2n_L$ and its elements are

$$\mathcal{J}_{\mu\nu}=\delta_{\mu\nu}-\frac{S(S+1)}{3k_BT_c}\mathcal{E}(|\mu-\nu|). \tag{15}$$

Due to the long-range summation occurring in $\mathcal{E}(|\mu-\nu|)$ [as seen from Eq. (10)], the critical temperature can be calculated from Eq. (14) only numerically. The formula given above can be approximated if we assume uniform magnetization distributions within each of the magnetic layers, i.e., when we substitute m_1 for the average magnetization in each atomic plane inside magnetic layer 1 and m_2 for layer 2, respectively. Then the critical temperature can be calculated from the approximate formula

$$k_BT_c=\frac{S(S+1)}{3}\frac{2\mathcal{E}_{\text{intra}}-n_L\mathcal{E}(0)\pm\mathcal{E}_{\text{inter}}}{n_L}, \tag{16}$$

where the "+" sign corresponds to the Curie temperature and is valid for ferromagnetic interlayer coupling ($E_{\text{inter}}<0$) while the "–" sign is for the Néel temperature and is valid when the magnetic layers are coupled antiferromagnetically ($E_{\text{inter}}>0$). The highest accuracy of uniform approximation (15) is for small magnetic layer thicknesses n_L.

When AF coupling exists between two magnetic layers, the mutual orientation of their magnetizations can be switched from antiparallel (antiferromagnetic) to parallel (ferromagnetic) one by applying an external magnetic field along the direction of their magnetizations. This kind of field-induced phase transition (*spin flop*) can take place below the Néel temperature.[39] The critical field H_c required to force the reversal of magnetization at $T\to 0$ can be determined by equating the total enthalpies of the system with FM and AFM orientation of magnetizations in the presence of that external field. The enthalpies are obtained from formula (6), which leads to the condition for H_c,

$$\mu_0H_c=\frac{|E_{\text{inter}}|}{g_{\text{eff}}\mu_BSNxn_L}. \tag{17}$$

The above expression can be written in the form more convenient for numerical calculations,

$$\mu_0H_c=B_0\frac{x}{n_L}\frac{|\mathcal{E}_{\text{inter}}|}{C}, \tag{18}$$

where

$$B_0=\frac{CS}{g_{\text{eff}}\mu_B} \tag{19}$$

is a material-dependent constant.

III. NUMERICAL RESULTS AND DISCUSSION

Since the existence and characteristic of RKKY interaction essentially depend on the electronic structure of the system under consideration, we make it a point of a brief discussion for the ultrathin film. The detailed description of the electronic structure of an ultrathin film, based on dispersion relation (1), is presented in Ref. 36, where especially the Fermi wave vector k_F and τ_F as well as the Fermi energy E_F were determined as functions of film thickness and charge-carrier concentration. In Fig. 2, the crucial quantity for studies of electronic properties, namely, the density of states (DOS) at Fermi level is plotted against the number of monolayers which make up the whole film. The DOS at Fermi level is, by definition, given by $\text{DOS}(E_F)=dN_c/dE_F$, and the method of its rather lengthy calculation for an ultrathin film has been presented in detail in Ref. 36. In further studies we make use of a normalized charge-carrier concentration $\rho=n_cd^3$. In the main plot, it is assumed that the number of charge carriers in the film is fixed and their normalized concentration equals $\rho=x/n$; thus, carrier concentration decreases when the film is made thicker. This assumption corresponds to the situation in which only two out of n atomic planes contain impurities which serve as charge donors, and the concentration of impurities within each doped plane is equal to x. Three impurity concentrations were selected, namely, $x=0.025$, 0.050, and 0.075 all belonging to the physically relevant range in DMS. For the inset we chose constant $\rho=x/2$, which is valid when all the atomic planes are doped with concentration x. For convenience, the values

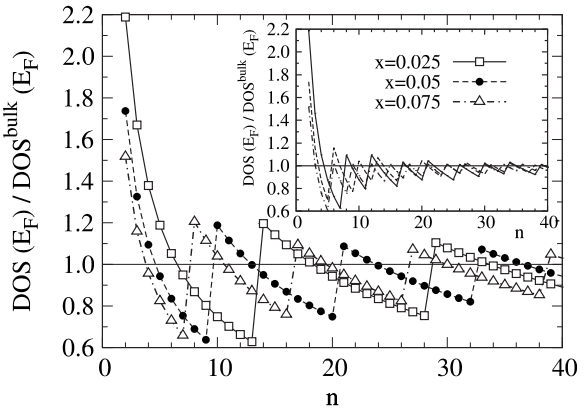

FIG. 2. Density of states at the Fermi level in an ultrathin film, normalized to the bulk value, as a function of number of monolayers. The charge-carrier concentration is assumed to be $\rho=x/n$ for three representative values of x. In the inset, a similar plot is shown for the charge-carrier concentration $\rho=x/2$.

of DOS were normalized to the corresponding values for the bulk case (for the appropriate value of ρ).

It is visible that DOS undergoes discontinuous jumps at some values of n. This is clear manifestation of quantum size effects (QSEs) as each of the jumps occurs for the charge-carrier concentration at which the next energy subband becomes occupied by the carriers, starting from a single 2D-like subband for the lowest concentrations. Although ρ is inversely proportional to the film thickness, the number of occupied energy subbands increases while increasing n. The distance between subsequent jumps becomes shorter by increasing the concentration x of charge-carrier donors. Between the jumps, normalized DOS decreases as $n^{-2/3}$. This reflects the fact that for a thin film the total DOS is a sum of (equal) contributions from each occupied 2D-like subband, and its value per surface unit of the film is given by the formula

$$\mathrm{DOS}(E) = \frac{m}{\pi\hbar^2}\sum_{\tau=1}^{\infty}\Theta\left(E - \frac{\hbar^2}{2m}\frac{\pi^2}{D^2}\tau^2\right), \tag{20}$$

where $\Theta(x)$ denotes the Heaviside step function. The 2D-like DOS per one charge carrier is energy independent so that dividing it by the 3D DOS per one charge carrier (proportional to $\rho^{-2/3}$) yields this behavior. The dependence presented in the main plot in Fig. 2 is a result of interplay between the changes caused solely by the change in quantum-well width and by decrease in the carrier concentration when the film becomes thicker. In the inset, for constant carrier concentration, we observe that the magnitude of QSE tends to vanish more rapidly for thicker films. For the film thicknesses n for which QSE manifest, we can expect similar discontinuous behavior of other physical properties which depend crucially on the DOS at the Fermi level.

Having a special case of formula (10) for $n_L=1$ (as in Ref. 32), we can study the interplanar coupling energies $\mathcal{E}(\Delta z/d)$. In formula (11), the summation of exchange integrals over the in-plane coordination zones has to be performed. Some cutoff radius must be assumed, large enough to assure satisfactory convergence of $\mathcal{E}$. It should also be emphasized that calculating each value of exchange integral $J(r_k,\omega d)$ constitutes a remarkable numerical task itself. Therefore, a noticeable computational effort is required to study the inter- and intralayer interaction energies so that we performed our calculations on the multi-CPU cluster. We performed the summation up to $k=1000$ coordination zones (which corresponds to the cutoff radius $r/d=82.0$ for even interplanar distances and $r/d=86.8$ for odd interplanar distances). In addition, we applied some averaging intended to remove the component oscillatory in cutoff radius. Such a procedure provides sufficient convergence of the resulting energies. Let us emphasize that accepting a finite spatial extension of interaction potential (2) is necessary to obtain finite interplanar coupling since the formulas contain the exchange integral $J(0,z)$ which would be divergent otherwise. In further calculations we assumed $\sigma/d=0.35$, which could correspond to 1 Å for (Ga,Mn)As (which we assume to be a realistic estimate of the spatial extension of d orbital carrying the localized spin).

It is interesting to follow the evolution of the energy dependence on interplanar distance when the film thickness n increases. We make an assumption that the charge-carrier concentration is $\rho=x/n$. In Fig. 3 we present $\mathcal{E}(\Delta/d)$ as being dependent on interplanar distance for various n and for $x=0.05$. It is remarkable that all the curves are symmetric with respect to the center of the film, i.e., $\mathcal{E}(\omega)=\mathcal{E}(n-\omega)$. It is a result of the similar symmetry of the RKKY coupling integral in ultrathin film (note that the symmetry properties of a RKKY coupling for a thin film have been mentioned first in the work of Wojtczak[40]). Let us remember that the summation over coordination zones within the atomic plane can be performed using the two sets of coordination radii and coordination numbers different for odd and even values of ω. However, for low values of charge-carrier concentration the inverse of the Fermi wave vector is quite large, and we are in the quasicontinuous regime so that the detailed lattice structure in the atomic plane is not of great importance. Thus, the symmetry $\mathcal{E}(\omega)=\mathcal{E}(n-\omega)$ is exact for every value of ρ only for n even, while it is approximate for low ρ for n odd.

In view of the experimental data, it might be instructive to mention that the constant C/a^2 approximately amounts to 1.6 $\mathrm{mJ/m^2}$ for (Ga,Mn)As. Therefore, for $x=0.05$ and $S=5/2$, the unit value in Figs. 3–6 presenting the coupling energy would correspond to 50 $\mu\mathrm{J/m^2}$.

It is visible that for $n=5-9$, the interplanar couplings are ferromagnetic (F) for the whole range of distances (with an exclusion of very weak antiferromagnetic (AF) values for $n=9$, near the center of the film). When n increases from 5 to 9, the coupling values are reduced continuously but the shape of the curve remains essentially unmodified. When n is changed from 9 to 10, a QSE is visible (compare Fig. 2). Thus, the curve shape changes discontinuously with two minimas, separated by a central maximum. The coupling values are at the same time shifted toward stronger ferromagnetic values. Then, further increase in n causes the gradual lowering of couplings, and for $n=16$ the two minima become AF in character. They reach the maximum depth for $n=20$. Switching to $n=21$, the next manifestation of QSE is visible as the curve develops an additional central minimum between two maximas. Once more, the coupling values became

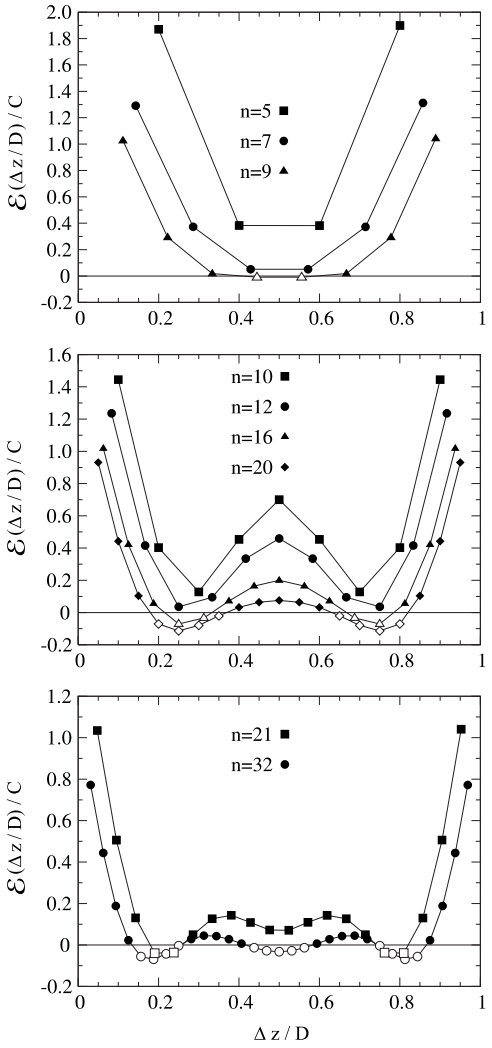

FIG. 3. Interplanar coupling energy for an ultrathin film containing n monolayers, as a function of separation between the planes, for the charge-carrier concentration $\rho=x/n$ and $x=0.05$.

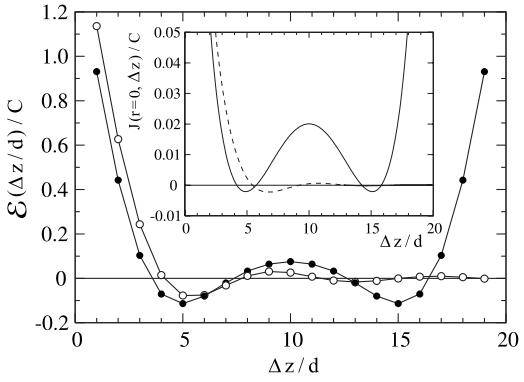

FIG. 4. Interplanar coupling energy in an ultrathin film for $n=20$, $x=0.05$, and the charge-carrier concentration $\rho=x/n$. Full points denote the values obtained from summation of the RKKY thin-film-modified exchange integral. The empty points represent the values obtained from summation of the usual RKKY bulk formula. In the inset, the very exchange integrals $J(r=0,z)$ are plotted: the solid line is for the RKKY interaction in thin film, while the dashed line corresponds to the bulk 3D RKKY coupling.

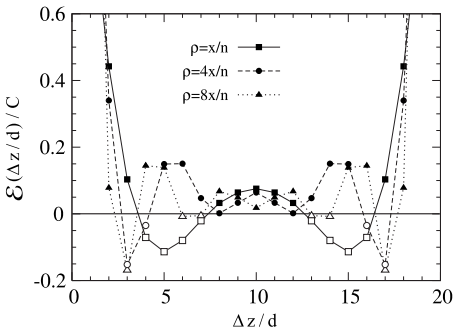

FIG. 5. Interplanar coupling energy for an ultrathin film characterized by $n=20$ and $x=0.05$ and for three representative charge-carrier concentrations.

shifted toward F, and the two AF minimas become shallower. When increasing n up to $n=32$, we notice the same tendency as before, namely, the couplings are lowered, the central minimum becomes AF in character, and the AF couplings near the two other minimas tend to rise.

It is instructive to compare the values of interplanar energy obtained by performing the summation in formula (10) for the thin-film RKKY coupling integral [given by Eq. (4)] with the some summation for the ordinary 3D RKKY coupling (with the same nonzero width of contact potential).[31] The results are presented in Fig. 4 for $\rho=x/n$, $n=20$, and $x=0.05$. The full circles correspond to the results derived from thin-film RKKY coupling, while the empty circles depict the interplanar coupling for 3D RKKY integral. It is visible that for the distances smaller than half of film thickness, the 3D coupling values are shifted toward F coupling, and also some phase shift is present. The curve for 3D RKKY does not possess the symmetry with respect to the center of the film so that it vanishes quite fast for $z/d>0.5$, unlike the proper thin-film RKKY coupling. In the inset of Fig. 4, the values of the exchange integral itself for $r=0$ for ultrathin film (solid line) and bulk 3D (dashed line) are plotted as a function of the distance z between the interacting spins. Here one can easily observe the phase shift and the difference in magnitudes between the two curves.

The interlayer coupling energy for $n_L=1$, calculated on the basis of formulas (8) and (10) is a key point in our study.

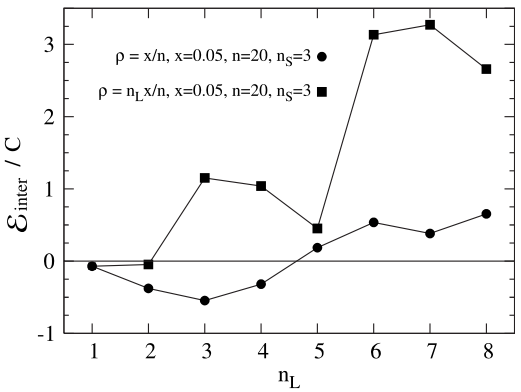

FIG. 6. Interlayer coupling energy for the system characterized by $x=0.05$, $n=20$, and $n_S=3$ as a function of magnetic layer thickness. The two charge-carrier concentrations: $\rho=x/n$ (circles) and $\rho_L x/n$ (squares) are assumed.

Knowing the interplanar coupling energies as a function of concentration of carriers and geometry of the ultrathin film, it is possible to search for the sets of parameters which result in the most robust antiferromagnetic interlayer coupling. As can be seen from formula (10), the interlayer energy is calculated by summing the interplanar coupling energies for $2n_L-1$ interplanar distances, ranging from $(n_S+1)d$ up to $(2n_L+n_S-1)d$, with appropriate weights. Therefore, if the maximum number of $\mathcal{E}(z)$ values, starting from $z=(n_S+1)d$, is antiferromagnetic, the strongest antiferromagnetism can be expected. On the other hand, since the coupling for $z=(n_S+1)d$ enters the sum in Eq. (10) with the largest weight n_L, it is also advisable to select n_S in order to have this AF coupling considerably strong. For example, from the analysis of Fig. 3, prepared for $x=0.05$, we can expect to obtain the AF interplanar coupling for the first minimum when we select $n_S=3$ for $n=20$. For thicker films, $n=32$, the optimum value seems to be $n_S=4$ (the first minimum) and $n_S=14$ [minimum in the middle, noticing that for $n_S=13$ the most important coupling $\mathcal{E}((n_S+1)d)$ would be only slightly antiferromagnetic]. For the larger number of subsequent antiferromagnetic values for $\mathcal{E}(z)$, we expect the stability of AF interlayer coupling for thicker magnetic layers. This thickness is of importance for two reasons. For one thing, with a diluted system in mind, the larger n_L means larger value of total magnetization; for another, maximizing the critical temperature is also advantageous. On the other hand, it appears that the increase in the concentration of charge carriers in the system would cause the antiferromagnetic behavior to diminish. This is due to the fact that the distance between the subsequent zeros of the function $\mathcal{E}(z)$ decreases when ρ increases so that the function oscillates more rapidly and the chance of having AF couplings for a few subsequent interplanar distances z decreases. Let us note that the last observation seems to stand in apparent contradiction to the general idea that for small concentration of charge carriers ferromagnetism is favored (because the first zero of the exchange integral is shifted toward larger distances and more coordination zones belong to this ferromagnetic range).

This effect is illustrated in Fig. 5, where the interplanar couplings are plotted for three charge-carrier concentrations: $\rho=x/n$, $\rho=4x/n$, and $\rho=8x/n$ for $n=20$ and $x=0.05$. It might be useful to mention here that these values for (Ga,Mn)As would correspond to the (physically relevant) hole concentrations of 1.1, 4.4, and 8.9×10^{20} cm^{-3}, respectively. It is clearly visible that for the lowest concentration of charge carriers, the antiferromagnetic minima are quite remarkable. When ρ is increased fourfold or eightfold, the oscillations of coupling versus interplanar distance become much faster so that only two or one coupling is of distinct AF character.

Figure 6 illustrates the magnetic layer thickness dependence of the interlayer coupling energy for the already mentioned case of $x=0.05$, $n=20$, and $n_S=3$. The coupling energy is plotted for two different carrier concentration regimes. The circles correspond to the constant carrier concentration of $\rho=x/n$, independent of the thickness of the magnetic layers n_L. The second result, marked by squares, is for the carrier concentration $\rho_L x/n$ proportional to the number of magnetically doped atomic planes. It can be seen that for the second case, the initial antiferromagnetic interlayer coupling energy is lost soon when n_L increases. Although the changes are strongly nonmonotonic, the AF coupling is never restored. The situation is very different for the constant charge-carrier concentration. The AF coupling persists up to $n_L=4$ and reaches the maximum strength for $n_L=3$. Further increase in magnetic layer thickness also leads to change to F interlayer coupling. The similar behavior can be observed for another sets of parameters regarded as beneficial in terms of assuring persistent AF interlayer coupling.

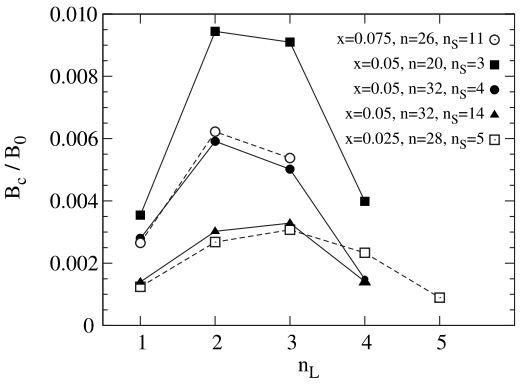

FIG. 7. External magnetic field required to switch the magnetizations of the layers from AF to F state as a function of layer thickness. The results are presented for $T\rightarrow0$ and selected parameters, where AF interlayer coupling is predicted.

Figure 7 presents the critical external field $B_c=\mu_0 H_c$ required to switch the direction of layer magnetizations from antiferromagnetic to ferromagnetic with temperature $T\rightarrow0$. The values have been calculated from formula (18) for the parameters predicting the strongest antiferromagnetic interlayer coupling. In order to provide some reference point, we calculated the value of a normalization constant B_0 [Eq. (19))] for a representative DMS, (Ga,Mn)As, which equals $B_0\simeq67$ T, so that the critical fields would lie in the range of hundreds of milli-Teslas. It is visible that the critical field for each case considered is largest for the magnetic layer thickness of $n_L=2$ or 3. If the lowest value of critical field is needed, together with the highest Néel temperature, then the best choice seems to be the maximum thickness of the magnetic layer which still provides AF interlayer coupling.

In connection with the predictions of Fig. 7, we would like to mention that an attempt to switch the magnetization direction in antiferromagnetically coupled multilayer of GaAs/(Ga,Mn)As has been made by Chung *et al.*[27] In their experiment, the field necessary to reverse the magnetization has been estimated at about 10 mT (judging from the magnetization curve and neutron reflectivity data); however, the full ferromagnetic alignment has not been achieved until 100 mT. It is worth noticing that in the experiment of Chung *et al.*[27] the spacer thickness was 12 ML, and each magnetic layer was 25 ML thick.

In the studies of critical temperature of the system, it was necessary to accept a specific spin value. Therefore, we selected $S=5/2$, which is relevant for DMS. The behavior of critical temperature of the system for the parameters leading

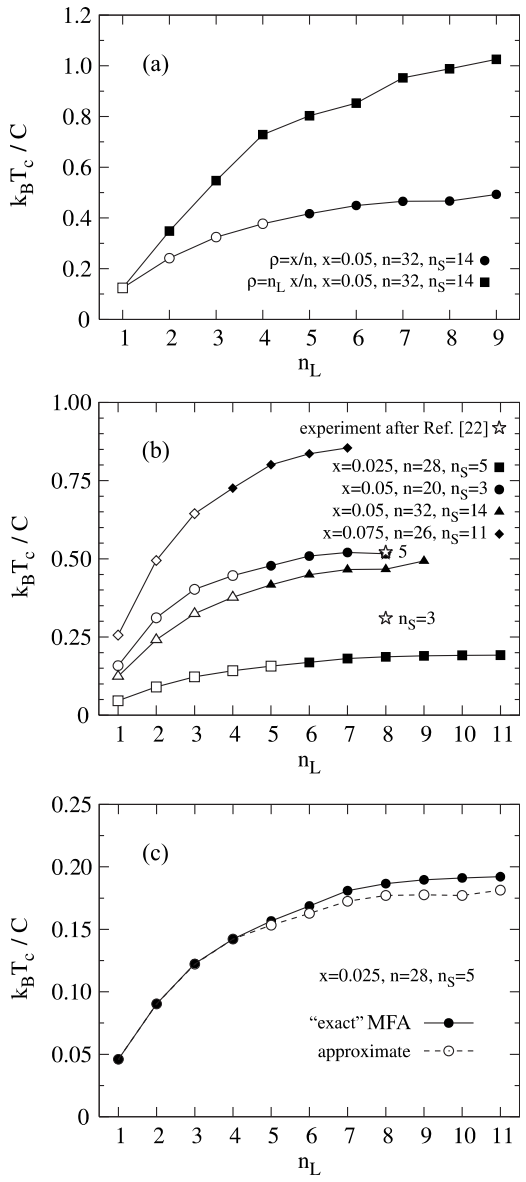

FIG. 8. Critical temperatures in MFA approximation for an ultrathin film with two magnetic layers. In (a) and (b) the filled symbols denote the Curie temperatures, while the empty ones are for the Néel temperatures. (a) Comparison of the results for charge-carrier concentration $\rho_L x/n$ (squares) and $\rho=x/n$ (circles). (b) Results for $\rho=x/n$ and various parameter ranges which are advantageous for AF interlayer coupling. (c) Comparison of the results obtained from the approximate [Eq. (15)] (empty symbols) and without this approximation (filled symbols).

to AF interlayer coupling is presented in Fig. 8(a). There, we plot the values of the critical temperatures for $x=0.05$, $n=32$, and $n_S=14$. Like in Fig. 5, the circles correspond to constant charge-carrier density $\rho=x/n$, while the squares are for $\rho_L x/n$. The empty symbols indicate the Néel temperatures (what corresponds to AF interlayer coupling), while the full symbols are for Curie temperature (F coupling). It is visible that for fixed ρ, the critical temperature tends to saturate when increasing n_L and reaches approximately constant value for the magnetic layer consisting of several ML. It is seen that the Néel temperature for $n_L=4$ is very close to that saturated value. For $\rho_L x/n$, the critical temperatures are mostly Curie temperatures and rise relatively fast when the magnetic layer thickness increases.

In order to investigate more carefully the critical temperatures for the regime of fixed charge-carrier concentration $\rho=x/n$, we perform the calculations for some other sets of parameters advantageous to AF coupling. The results are presented in Fig. 8(b). The same tendency for the critical temperature to saturate for thick magnetic layers is observed, and the maximum values of Néel temperature lie close to that limit of saturation.

Let us mention that a similar behavior of Curie temperature for thin films with RKKY interaction has been found in the Monte-Carlo-based studies of Boselli *et al.*[16] for fixed charge-carrier concentration. However, they considered a thin film with magnetic impurities distributed randomly in all the atomic planes and their study was focused mainly on noncollinear magnetic phases, resembling canted ferromagnetism.

For (Ga,Mn)As, the value of energy constant C/k_B would be approximately 36 K. In Fig. 8(b), two experimental values were depicted, taken from the paper of Mathieu *et al.*,[22] obtained for (Ga,Mn)As with $x=0.04$ for $n_L=8$ and two values of $n_S=3$ and 5. It must be strongly emphasized that these values of Curie temperature were measured for a superlattice geometry, not for a trilayer, and the charge-carrier concentration for the sample was not known. Therefore, they are shown here merely to indicate that the order of magnitude of estimated Curie temperatures for a trilayer is in reasonable agreement with the available superlattice data.

Figure 8(c) compares the critical temperature calculated from the "exact" MFA formula [Eq. (14)] and from approximate formula (16) as being dependent on magnetic layer thickness for the set of parameters $x=0.025$, $n=28$, and $n_S=5$. It can be concluded that the assumption of uniform magnetization distribution inside each magnetic layer does not lead to a noticeable change in the critical temperature for the layers up to 4 ML thick. However, for thicker layers, the critical temperature is underestimated by an approximate formula on the order of 5%, which holds also for other sets of parameters.

It follows from the numerical calculations that the intralayer energy is much larger than the absolute value of the interlayer coupling. As a consequence, it is clearly visible from Eq. (16) that the main contribution to the critical temperature originates from $\mathcal{E}_{\text{intra}}$.

As mentioned previously, in the ordered state, each atomic plane of the magnetic layer has its own magnetization value and some nonuniform magnetization distribution exists across the layer thickness. To illustrate this behavior, we calculated such magnetization profiles for various thicknesses of the magnetic layers n_L for the cases of $x=0.05$, $n=32$, and $n_S=14$ [Fig. 9(a)] as well as for $x=0.025$, $n=28$, and $n_S=5$ [Fig. 9(b)]. The plots present a magnetization distribution in a single magnetic layer. Each profile is calculated for the temperature of $\frac{2}{3}T_c$ for the given value of n_L versus the number of the atomic plane counted starting from the plane situated closest to the undoped spacer. For the second magnetic

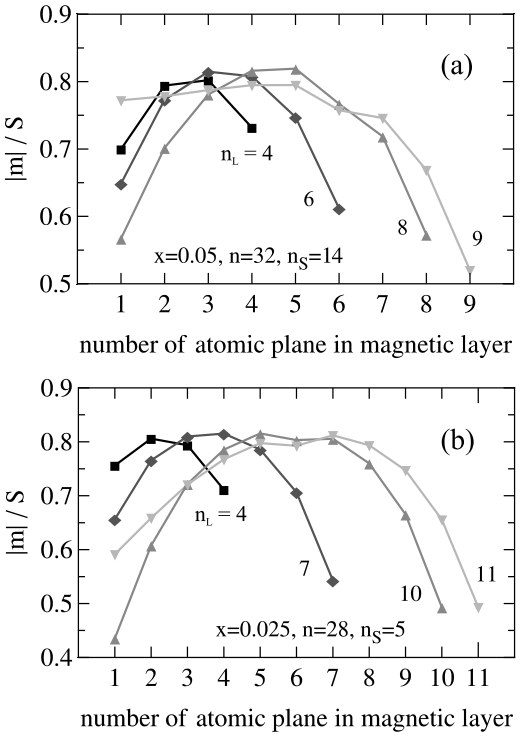

FIG. 9. Spatial distribution of magnetizations in subsequent monolayers for various thicknesses n_L and for two sets of parameters: (a) $x=0.05$, $n=32$, and $n_S=14$; and (b) $x=0.025$, $n=28$, and $n_S=5$. The temperature is $T=(2/3)T_c$.

layer, the values of m are either the same (for F interlayer coupling) or they are of opposite sign (for AF coupling) so that the profile is either symmetric or antisymmetric with respect to the center of the undoped spacer. It is noticeable that for small thicknesses, $n_L=2$, the distribution is almost uniform, while the increasing thickness of the magnetic layer causes the profile to reshape. The maximum of magnetization occurs for the atomic plane in the middle of the magnetic layer, while the smallest values are reached for the planes which are the most distant or the closest to the nonmagnetic spacer. For $n_L=8$ in Fig. 9(a) or $n_L=10$ in Fig. 9(b), the distribution is approximately symmetric with respect to the middle atomic plane in the layer. It is noticeable that the differences in magnetizations for various atomic planes are strongly evident since the magnetization at the boundaries of the magnetic layer is only a half of the maximum value reached in its center. Interestingly, the profile loses its symmetry when we reach the maximum of possible magnetic layer thickness, $n_L=9$ for (a) and $n_L=11$ for (b). Then the magnetization value in the atomic planes in the vicinity of the spacer is enhanced in comparison with the layers at the opposite side of the magnetic layer. Such an effect is more striking for the set of parameters $x=0.05$, $n=32$, and $n_S=14$, where the distribution of magnetization switches from almost symmetric shape with respect to the middle plane of the layer (for $n_L=8$) to almost flat one with some drop at high distances from the spacer (for $n_L=9$). By approaching the critical temperature the profiles flatten and their magnitude vanishes.

IV. FINAL REMARKS AND CONCLUSION

The analysis of a model magnetic bilayer with ultrathin-film-modified RKKY interaction revealed an importance of QSE for obtaining antiferromagnetic interlayer coupling. Some ranges of parameters, advantageous for AF, were identified with the general remark that the carrier density should not be as high as to make the oscillation period excessively short. The coupling is possible even for relatively thick spacers (14 ML, for example); however, the maximum thickness of each magnetic layer should not exceed a few ML. The critical temperatures were found to saturate their values when increasing magnetic layer thickness.

The general conclusion which can be drawn from the study is that the occurrence of AF coupling presents a quite unique situation in comparison with the most common F ordering. It might be deduced from the theoretical works concerning the multilayers[12–14] that the AF interlayer coupling might seem present in a relatively wider range of charge-carrier concentrations (what has been noticed in a recent review in Ref. 41, as contrasting with the experimental confirmations of robust ferromagnetic behavior). In trilayers, the interlayer coupling sign results from a rather subtle interplay of quantum size effects and the tendency for exchange integrals to shift toward ferromagnetic coupling, which is dominant for ultrathin quantum-well systems. Thus, in order to observe the AF configuration the special set of parameters has to be chosen including the impurity concentration, its distribution within the thin film, the thickness and the carriers density. Some exemplary sets of the parameters, including dopant and charge-carrier concentration, thicknesses of the film, and magnetic layers, can be seen in Figs. 8(a) and 8(b), denoted there by empty markers. Studies of sensitivity of the obtained AF configuration to the external magnetic field might be useful for practical realization of the switching function between the AF and F states. Let us also mention that Ref. 41 points out that for unambiguous experimental detection of AF interlayer coupling, the ability of performing single layer-resolved measurements is vital. Such experiments appear especially accessible in trilayers (see, for example, Ref. 24). In general, the trilayer system appears as the fundamental one from the point of view of understanding the physics of interlayer coupling.

A comparison of our thin-film RKKY approach with other theoretical models, for instance with the $\mathbf{k}\cdot\mathbf{p}$ kinetic exchange model,[12] or tight-binding approximation,[13] is not a straightforward task because those models were studied for the superlattice systems. It is worthy to emphasize here the fundamental difference between the geometries of trilayer (or magnetic bilayer) used in our studies and superlattice. In the case of a superlattice, the periodicity along the direction perpendicular to the structure plane occurs, which is reflected by the Bloch-like form of the carrier wave function in quasi-1D potential. The electronic structure, consisting of minibands (dependent on the localized spins orientation), is then a subject of calculations yielding the interlayer coupling energy. If no band shift at the interfaces is assumed, the superlattice system would appear equivalent to a single quantum well with a very large width (what would result in disappearance of noticeable quantum size effects). On the

contrary, for a trilayer, the boundary conditions require the wave function to vanish outside of the well, which gives rise to the pronounced quantum size effects. Within the limit of large total thickness of the multilayer, the ordinary 3D-like form of the RKKY interaction would be restored. Therefore, it is difficult to make direct comparison between the theoretical predictions for both mentioned sample geometries. This would require a separate calculation devoted to the multilayer geometry and might be a subject of a future work.

However, some comments on the physics captured by the models can be made. In the case of the $\mathbf{k}\cdot\mathbf{p}$ kinetic exchange model[12] the Fermi wave vector has been assumed in the bulk approximation, whereas in our model it is dependent on the quantum-well structure.[36] Also the RKKY exchange integral is not assumed here in a quasi-1D form (as in the case of superlattices) but is strictly characteristic for the thin film. As a result, for the energy calculation in the thin film a numerical summation of the exchange integrals can be made, which we believe in this case is the most proper method. It could also be useful for other molecular-field-like approaches.[14] More importantly, the periodicity of the interlayer energy coupling resulting from summation is not the same as the periodicity of the exchange integral itself.

Regarding the tight-binding method,[13] the results obtained for multilayers were very weakly sensitive to the magnetic layer thickness, which is not the case in our quantum-well model. The strong difference can also be predicted in the limit of vanishing charge-carrier concentration. In such case the RKKY exchange integral tends to zero, while the interlayer coupling mediated by valence-band electrons in the tight-binding model can have finite value.

Several of our results are in agreement with MC simulations by Boselli *et al.*[16] made for the quantum well. This concerns, for instance, the ferromagnetic state for the layers which has been obtained from the intralayer energy. Also, the observation that the intralayer energy is several times larger than the interlayer coupling has been confirmed by present findings. However, the antiferromagnetic coupling has not been found there;[16] instead, the canted phase has been reported for individual samples. Unfortunately, the contact potential assumed for this MC simulation, as well as in other works,[17] has been the Dirac's δ function. We think that the Gaussian distribution, with some nonzero dispersion of the order $\sigma \sim 1$ Å assumed in this work, reflects more properly the spatial extension of the localized magnetic orbitals.

As mentioned before, our approach is based on the RKKY perturbational formalism generalized to account for the band structure discretization in a single quantum well so that it shows clearly the importance of quantum size effects. We are convinced that this makes the method particularly useful for studying the trilayers. Especially, there exists a clear correlation between the noncontinuous behavior of the density of states at the Fermi level and the coupling energy. In particular, for the trilayers, the key to obtaining the antiferromagnetic interlayer coupling is making use of the quantum size effects as the strongest AF interactions correspond to the situation where energy subbands are almost completely filled by charge carriers. This behavior is characteristic of a trilayer, constituting a narrow quantum well, and might not be expected for multilayer samples.

However, it should be kept in mind that the model reflects only partially the features of real thin-film DMS systems, especially related to the exact band structure or shape of the confining potentials as well as the strength of the coupling between the carriers and localized spins. On the other hand, the results we obtain seem to be realistic in light of the experimental results mentioned in the previous section (concerning the interlayer coupling energy, the Curie temperature or the critical external field). It might be worth noticing that the critical temperatures observed by Mathieu *et al.*[22] for superlattices consisting of 8 ML of (Ga,Mn)As and undoped spacers of $3,\ldots,9$ ML were between 10 and 20 K (what resembles the order of temperatures predicted for our ultrathin trilayer structures). As a rule, the samples possessing a trilayer geometry studied so far experimentally were characterized by noticeably thicker magnetic layers than the structures we consider. On the other hand, let us mention that recently the ferromagnetic transition at about 30 K has been observed even in ultrathin films of (Ga,Mn)As just 2 nm thick (i.e., consisting of 7 ML).[42] The critical temperature for thicker annealed films, up to 5 nm, was approximated as high as 100 K.[43]

Since our method is based on summation of the thin-film-modified RKKY coupling between each pair of spins in the system, it does not rely on the pseudo-1D RKKY approach. Instead, it offers the possibility to separate the inter- and intralayer components of interaction and enables the analysis of various thermodynamic properties. Owing to that, it might allow for straightforward handling of the subject of interface roughness caused by diffusion of magnetic impurities into the undoped region, a problem which is also interesting in studies of multilayers. Thus, the sensitivity of the coupling to the spacer thickness selection might be important from the point of view of the interface roughness. Moreover, in the present work it has been assumed that the (random) positions of the magnetic impurity ions are uncorrelated. However, it could be also possible to investigate the influence of correlated positional disorder on the magnetic properties of the thin-film systems by considering the nonzero Warren-Cowley parameter within the formalism developed.

The magnetization profiles in thin films were already studied for nearest-neighbor interactions a long time ago;[8,44,45] for the long-range RKKY interactions the analogous profiles are presented here. The prediction of the profiles would need some experimental confirmation in the future studies of DMS systems. Let us observe that the presence of nonuniform magnetization profile causes a noticeable decrease in the total magnetization of each magnetic layer at finite temperatures (with respect to the prediction of the usual, bulk Brillouin function).

In an ultrathin film, the characteristic features of RKKY exchange integral depend crucially on the standing-wave form of the free-carrier wave functions. They originate from the interference of waves propagating perpendicularly to the thin-film plane. Thus, an adequate phase coherence length for free charge carriers is required for this picture to be valid. Taking (Ga,Mn)As as an example, the coherence lengths of the order of 100 nm have been reported in quantum wires and rings for milli-Kelvin temperatures (in the presence of

magnetic impurities),[46] even though a mean-free path for the carriers is shorter, down to an order of a lattice constant in the metalliclike regime.[43] Such a value of phase coherence length exceeds the thicknesses of the films presented in this paper.

ACKNOWLEDGMENTS

We gratefully acknowledge computational support on HUGO cluster at Department of Theoretical Physics and Astrophysics, P. J. Šafárik University in Košice (with the help of M. Jaščur and Z. Kuscsik).

*kszalowski@uni.lodz.pl

[1] P. Grünberg, R. Schreiber, Y. Pang, M. B. Brodsky, and H. Sowers, Phys. Rev. Lett. **57**, 2442 (1986).
[2] P. Grünberg, J. Magn. Magn. Mater. **226-230**, 1688 (2001).
[3] P. Bruno, J. Phys.: Condens. Matter **11**, 9403 (1999).
[4] J. Barnaś, Phys. Rev. B **52**, 10744 (1995).
[5] M. Sapozhnikov and G. Genkin, J. Magn. Magn. Mater. **139**, 179 (1995).
[6] V. Dugaev, V. Litvinov, W. Dobrowolski, and T. Story, Solid State Commun. **110**, 351 (1999).
[7] D. M. Edwards, J. Mathon, R. B. Muniz, and M. S. Phan, Phys. Rev. Lett. **67**, 493 (1991).
[8] I. Staniucha and A. Urbaniak-Kucharczyk, Phys. Status Solidi C **3**, 65 (2006).
[9] J. Fabian, A. Matos-Abiague, C. Ertler, P. Stano, and I. Žutić, Acta Phys. Slov. **57**, 565 (2007).
[10] A. Fert, Thin Solid Films **517**, 2 (2008).
[11] T. Dietl, A. Haury, and Y. M. d'Aubigné, Phys. Rev. B **55**, R3347 (1997); T. Dietl, J. Cibert, D. Ferrand, and Y. M. d'Aubigné, Mater. Sci. Eng., B **63**, 103 (1999).
[12] A. D. Giddings, T. Jungwirth, and B. L. Gallagher, Phys. Status Solidi C **3**, 4070 (2006); Phys. Rev. B **78**, 165312 (2008).
[13] P. Sankowski and P. Kacman, Phys. Rev. B **71**, 201303(R) (2005).
[14] T. Jungwirth, W. A. Atkinson, B. H. Lee, and A. H. MacDonald, Phys. Rev. B **59**, 9818 (1999).
[15] S. C. P. Rodrigues, L. M. R. Scolfaro, J. R. Leite, I. C. da Cunha Lima, G. M. Sipahi, and M. A. Boselli, Phys. Rev. B **70**, 165308 (2004).
[16] M. A. Boselli, I. C. da Cunha Lima, and A. Ghazali, Phys. Rev. B **68**, 085319 (2003).
[17] M. A. Boselli, I. C. da Cunha Lima, and A. Ghazali, J. Appl. Phys. **85**, 5944 (1999); **87**, 6439 (2000); M. A. Boselli, L. L. da Silva, I. C. da Cunha Lima, and A. Ghazali, *ibid.* **93**, 6790 (2003).
[18] J. Sadowski *et al.*, Thin Solid Films **412**, 122 (2002); J. Sadowski, R. Mathieu, P. Svedlindh, J. Kanski, M. Karlsteen, K. Świątek, and J. Domagała, Acta Phys. Pol. A **102**, 687 (2002); C. Hernandez, F. Terki, S. Charar, J. Sadowski, D. Maude, V. Stanciu, and P. Svedlindh, *ibid.* **103**, 613 (2003).
[19] N. Akiba, F. Matsukura, A. Shen, Y. Ohno, H. Ohno, A. Oiwa, S. Katsumoto, and Y. Iye, Appl. Phys. Lett. **73**, 2122 (1998).
[20] D. Chiba, N. Akiba, F. Matsukura, Y. Ohno, and H. Ohno, Appl. Phys. Lett. **77**, 1873 (2000); Physica E **10**, 278 (2001).
[21] K. Dziatkowski, Z. Ge, X. Liu, J. Furdyna, B. Clerjaud, and A. Twardowski, Acta Phys. Pol. A **112**, 227 (2007).
[22] R. Mathieu, P. Svedlindh, J. Sadowski, K. Świątek, M. Karlsteen, J. Kanski, and L. Ilver, Appl. Phys. Lett. **81**, 3013 (2002).
[23] W. Szuszkiewicz, E. Dynowska, F. Ott, B. Hennion, M. Jouanne, J. F. Morhange, and J. Sadowski, J. Supercond. **16**, 209 (2003); W. Szuszkiewicz, E. Dynowska, F. Ott, B. Hennion, M. Jouanne, J. F. Morhange, M. Karlsteen, and J. Sadowski, Acta Phys. Pol. A **100**, 335 (2001).
[24] B. J. Kirby, J. A. Borchers, X. Liu, Z. Ge, Y. J. Cho, M. Dobrowolska, and J. K. Furdyna, Phys. Rev. B **76**, 205316 (2007).
[25] A. Mikkelsen, L. Ouattara, H. Davidsson, E. Lundgren, J. Sadowski, and O. Pacherova, Appl. Phys. Lett. **85**, 4660 (2004); A. Mikkelsen and E. Lundgren, Prog. Surf. Sci. **80**, 1 (2005).
[26] Z. Ge, Y. Y. Zhou, Y.-J. Cho, X. Liu, J. K. Furdyna, and M. Dobrowolska, Appl. Phys. Lett. **91**, 152109 (2007).
[27] J.-H. Chung, S. J. Chung, S. Lee, B. J. Kirby, J. A. Borchers, Y. J. Cho, X. Liu, and J. K. Furdyna, Phys. Rev. Lett. **101**, 237202 (2008).
[28] J. König, J. Schliemann, T. Jungwirth, and A. MacDonald, in *Electronic Structure and Magnetism of Complex Materials*, edited by D. J. Singh and D. A. Papaconstantopoulos (Springer, New York, 2002).
[29] J. Schliemann, J. König, and A. H. MacDonald, Phys. Rev. B **64**, 165201 (2001); J. Schliemann and A. H. MacDonald, Phys. Rev. Lett. **88**, 137201 (2002); J. Supercond. **16**, 11 (2003); J. Schliemann, Phys. Rev. B **67**, 045202 (2003).
[30] L. Brey and G. Gómez-Santos, Phys. Rev. B **68**, 115206 (2003).
[31] K. Szałowski and T. Balcerzak, Phys. Rev. B **78**, 024419 (2008).
[32] K. Szałowski and T. Balcerzak, Acta Phys. Pol. A **114**, 1375 (2008).
[33] T. Balcerzak, Thin Solid Films **515**, 2814 (2006).
[34] T. Balcerzak, J. Magn. Magn. Mater. **310**, 1651 (2007).
[35] T. Balcerzak, in *Trends in Thin Solid Films Research*, edited by A. R. Jost (Nova Science Publishers, New York, 2007), Chap. 9.
[36] T. Balcerzak, Thin Solid Films **500**, 341 (2006).
[37] S. F. Edwards and J. M. Loveluck, J. Phys. C **3**, S261 (1970).
[38] K. Szałowski and T. Balcerzak, Phys. Rev. B **77**, 115204 (2008).
[39] L. Néel, Ann. Phys. (Paris) **5**, 232 (1936).
[40] L. Wojtczak, Acta Phys. Pol. **36**, 585 (1969).
[41] S. Lee, J.-H. Chung, X. Liu, J. K. Furdyna, and B. J. Kirby, Mater. Today **12**, 14 (2009).
[42] R. Gareev, A. Petukhov, M. Schlapps, M. Doeppe, J. Sadowski, M. Sperl, and W. Wegscheider, arXiv:0806.2590 (unpublished).
[43] B. S. Sørensen, P. E. Lindelof, J. Sadowski, R. Mathieu, and P. Svedlindh, Appl. Phys. Lett. **82**, 2287 (2003).
[44] L. Wojtczak, Czech. J. Phys., Sect. B **20**, 247 (1970).
[45] G. Wiatrowski, T. Balcerzak, L. Wojtczak, and J. Mielnicki, Phys. Status Solidi B **138**, 189 (1986).
[46] K. Wagner, D. Neumaier, M. Reinwald, W. Wegscheider, and D. Weiss, Phys. Rev. Lett. **97**, 056803 (2006); D. Neumaier, K. Wagner, U. Wurstbauer, M. Reinwald, W. Wegscheider, and D. Weiss, New J. Phys. **10**, 055016 (2008).